Investigation of the Structure and Stability of an Alcohol-Based Polymer for Hydrogen Storage in the Form of Ions

Hiroshi Matsuura,* Tamio Tanikawa, Shuichi Ushiba,[1] and Makoto Ogawa[2]

Intelligent Systems Institute, National Institute of Advanced Industrial Science and Technology, Tsukuba 305-8564

[1]IR/Raman Group, Spectroscopy Department, Thermo Electron, C-2F 3-9 Moriya-cho, Yokohama 221-0022

[2]Department Mechanical Engineering II, Shibaura Institute of Technology, Saitama 337-8570

Received June 8, 2004; E-mail: hiroshi-matsuura@aist.go.jp

This study reports on the structure and stability of an alcohol-based polymer, which stores hydrogen in the form of ions. The hydrogen-storing polymer is produced from alcohol using a plasma-induced method. Measurements of the electrical resistivity and the IR spectra of the polymer indicate that it is in an electrically unstable state. The hydrogen produced by the polymer following the application of an electric signal demonstrates that the hydrogen ions are trapped within the polymer. The development of hydrogen-storing techniques in the form of ions improves the controllable extraction of hydrogen.

In recent years, there has been increasing interest in methods for the production[1–3] and storage[4–6] of hydrogen. In most studies, these two issues have been investigated separately, with some researchers investigating methods for hydrogen production[1–3] and others investigating hydrogen-storage techniques, such as the use of carbon nanotubes.[7–9] Our current study[10] aims to address both of these issues, first by storing hydrogen in an ionic form in an alcohol-based polymer, and then producing hydrogen by applying electricity.

When hydrogen atoms in an alcohol solution are dissociated and trapped as ions in a polymer, they can be extracted from the polymer by electrical neutralization. A relatively stable state of the polymer is necessary for the storage of hydrogen ions, while a relatively unstable state is required for the extraction of hydrogen from ions electrically. Therefore, the condition of alcohol polymerization is an important factor for this strategy.

However, one of the difficulties in polymerizing alcohol is accurate control of the reaction conditions. In general, polymerization is achieved by controlling the temperature and pressure of the reaction.[11–13] However, this approach is problematic because alcohol is volatile, and therefore conventional approaches cannot be used. In addition, there are no catalysts known to facilitate the polymerization of alcohol. Therefore, it is necessary to apply different forms of energy to achieve the decomposition and rearrangement of molecules required for producing an alcohol-based hydrogen storing polymer.

In this study we used electron emission as a method for supplying energy to alcohol molecules. Our results showed that electron emission applied between different sized electrodes is an effective method for controlling the amount of emission energy delivered to the target molecules.

Results and Discussion

Dynamics of the Alcohol Polymerization. Figure 1 illustrates the dynamics of alcohol interacting with electron emission during the alcohol polymerization process. An electric potential was applied between an atomic force microscope (AFM) tip and the surface of liquid 1-butanol. Figure 1a depicts the AFM tip and the surface of 1-butanol prior to the application of an electric potential. When an electric potential of 0.8 kV–15 kHz was supplied, and the distance between the AFM tip and the surface of the 1-butanol was adjusted to 55 μm, an average electric current of 23 μA was achieved.

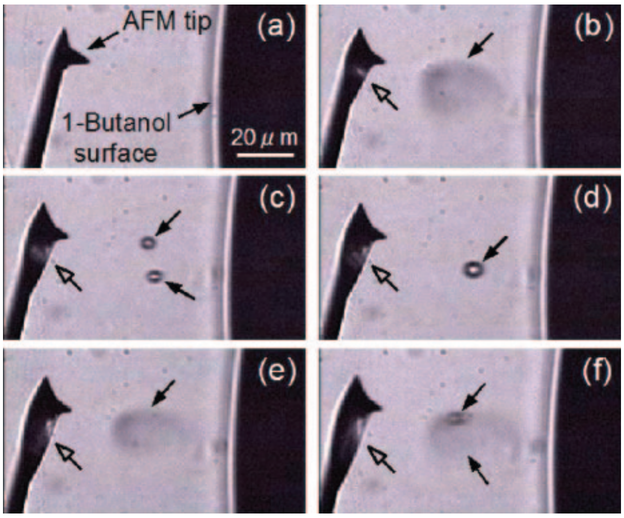

Fig. 1. Dynamics of alcohol interacting with electrons in an electric field. A nanoscale mist appeared between the electrodes as shown in (b). The mist condensed to form microscale particles (c). The particles were attracted toward each other and grouped together at a point between the two electrodes (d). The particles then re-formed into a mist (e). Figure (f) depicts the formation of a spherical particle from the mist (e). The transition of particles to mist continued until the AFM tip was completely covered with the mist.

Published on the web January 13, 2005; DOI 10.1246/bcsj.78.88

A nanoscale mist appeared soon after the application of an electric current (Fig. 1b). The mist was produced only in the region between the top of the AFM tip and the surface of the liquid 1-butanol. The mist was visible at the mid-point between the two electrodes. The time resolution of a video camera recorder (VCR) used to record the images was 30 Hz, and therefore a relatively clear image of the mist indicates that the mist remained in the same position over a time scale similar to the time resolution of the VCR (0.033 s).

The mist shown in Fig. 1b condensed into two spheres at the mid-point between the electrodes, as shown in Fig. 1c. The two spherical particles (Fig. 1c) combined to form a larger particle, as shown in Fig. 1d. This larger particle re-formed into a mist, as shown in Fig. 1e. The mist then re-condensed and formed a particle, as shown in Fig. 1f (black arrows). The unstable appearance of the alcohol indicated that the electric interaction between the alcohol molecules and the electrons emitted from the AFM tip occurred in the electric field.

The white arrows at the base of the AFM tip (Figs. 1b to 1f) show a gradual increase in the amount of mist and particles on the AFM tip. This suggests that the 1-butanol was transported from the 1-butanol surface toward the AFM tip. Furthermore, it was found that both the mist and the particles transported at the AFM tip were stable in air and under vacuum conditions. This indicates that the molecular structure of the 1-butanol was decomposed under the experimental conditions used in this study.

Apparatus Used to Achieve Alcohol Polymerization. The dynamics of alcohol polymerization shown in Fig. 1 was induced using the apparatus illustrated in Fig. 2. The most important feature of the apparatus is the use of a dielectric liquid. The simultaneous formation of a dielectric molecular current toward the AFM tip and electron emission toward the current from the AFM tip were important factors in the successive reactions that lead to producing the polymer (Figs. 2a, 2b). We assume in this paper that the volatile dielectric alcohol molecules would initially be attracted electrically from its surface toward the electrode, and the movement is called "a molecular current". In this study, alcohol was used as the hydrogen-storing polymer. However, it is likely that any dielectric liquid containing hydrogen atoms could be used to achieve the same result.

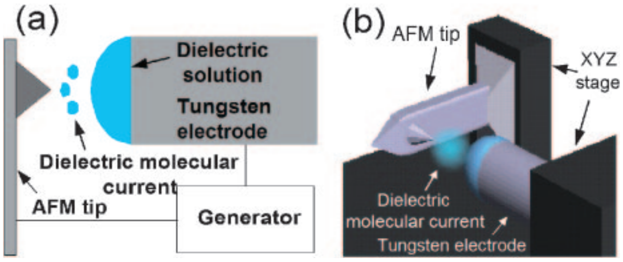

Fig. 2. Experiment apparatus used for the polymerization of dielectric organic compounds. (a) 2-Dimensional image of the apparatus. One of the important features of the apparatus was the use of a "liquid electrode" to form a dielectric molecular current between the electrodes. The current formed as a result of an electric interaction. (b) 3-Dimensional image of the apparatus. The electrodes were mounted on an XYZ-stage to accurately control their relative positions. The AFM tip (DF-20 SII) consisted of Au-coated silicon.

Figures 2a and 2b represent 2-D and 3-D images of the experiment apparatus. An AFM tip consisting of Au-coated silicon was used as a negative electrode. The side of a tungsten rod was used as a positive electrode. 1-butanol was applied to the side of the positive electrode, as illustrated in Fig. 2a. The negative AFM tip was placed 0.4 mm from the side of the positive electrode. The AFM tip was moved to a distance of 55 μm from the surface of the 1-butanol. The relative positions of the AFM tip and the tungsten rod were controlled by mounting the electrodes on an XYZ-stage (Fig. 2b).

An electric potential of 0.8 kV–15 kHz was applied between the electrodes. This induced a 23 μA electric current. The experiments were carried out in air at a temperature of 26 °C and a humidity of 50%.

Analysis of the Alcohol Polymerization Process. The polymerization of alcohol, as observed in Fig. 1, can be explained using the model shown in Fig. 3. This model shows the bombardment of electrons toward the electrically attracted alcohol in the electric field produced between different-sized electrodes (Fig. 3a). Alcohol was placed on the positive electrode, and a smaller electrode was used as the negative electrode. This pair of electrodes produced an asymmetrical electric field (black arrows, Fig. 3a).

The asymmetrical electric field played two important roles in the alcohol-polymerization process. First, this electric field generated a molecular alcohol current that flowed from the larger to the smaller electrode. Second, the smaller negative electrode allowed accurate control of the electron bombardment.

Figure 3b shows the molecular alcohol current (black arrows), from the surface of the alcohol on the positive elec-

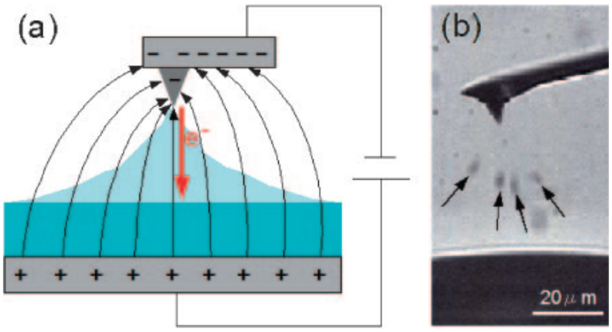

Fig. 3. Generation of a molecular alcohol current and simultaneous electron bombardment in the direction of the current. (a) The different sized electrodes resulted in a difference in the electric flux density. The density gradient of the electric lines of force generated an intense Maxwell tensor effect that resulted in the attraction of alcohol molecules toward the smaller electrode. The high density of the electric lines of force also caused electron bombardment directed toward the molecular alcohol current. (b) Optical image showing the generation of a molecular alcohol current flowing toward the smaller electrode (black arrows) and the simultaneous emission of electrons toward the current (not visible).

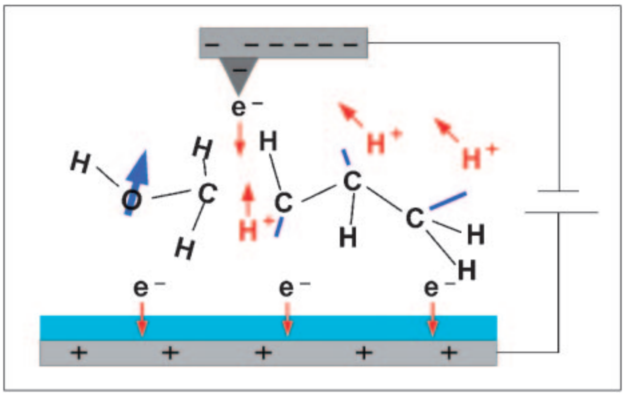

Fig. 4. Model of the molecular current and the dissociation of molecules. The asymmetrical electric field between the sharpened negative electrode and the positive electrode electrically attracted dielectric molecules toward the smaller electrode. The tip simultaneously emitted electrons toward the attracted molecules and dissociated the molecules during their collision in air.

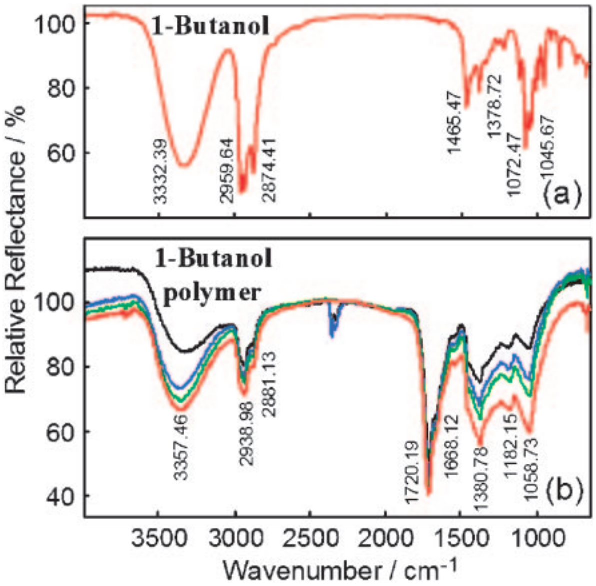

Fig. 5. Transition of the IR spectrum of the alcohol-based polymer. The stability of the polymer was investigated by recording the IR spectra at 30 min intervals.

trode, to the smaller negative electrode. The intense electric field at the tip resulted from the movement of the upward-flowing alcohol current (black arrows). The radial movement of the alcohol particles toward the tip of the smaller electrode indicated that the most intense electric field was generated at the tip of the electrode. From these observations, it is clear that the dielectric alcohol particles are attracted toward the tip, in the direction of the electric field. The permittivity of O–H bases in the alcohol molecules should have contributed to the generation of the molecular alcohol current as a result of an electric interaction with the asymmetrical electric field[14–16] (Fig. 4).

The dissociation process of 1-butanol molecules and successive alcohol polymerization, as outlined in Fig. 1, can be explained using the model shown in Fig. 4 as follows. The intense electric field near the top of the AFM tip generated electron emission, and simultaneously attracted the dielectric 1-butanol molecules toward the tip through a polarization interaction (Fig. 4). The electron bombardment into the 1-butanol molecular current directed toward the tip caused their collisions and successive dissociation of the molecules (Fig. 4). The dissociation of 1-butanol molecules lead to the production of positive and negative ions that immediately migrated toward the negative and positive electrodes, respectively (Fig. 4). An alcohol polymer was formed after electrical neutralization of these ions at the electrically opposite electrodes. The measured output electric current (2 µA) indicated that 21 µA of electrons were either consumed during the polymerization process or lost in the air (Fig. 4).

The collision or electrical interaction between the molecular current and electron emission played a critical role in the dissociation of molecules and the successive alcohol polymerization process. Since the kinetic energy of the emitted electrons inherently has some distributions, and the electrons randomly interact with the bonding of the molecules, the structures of the partially dissociated molecules should consist of various structures of ions and radicals. Therefore, it is likely that the polymer composed on the AFM tip would initially be electrically unstable (Fig. 1, white arrows). The unstable state of this polymer was observed by the transition of IR spectra with time.

Unstable State of the 1-Butanol Polymer. The decomposition of 1-butanol molecules and the stability of the polymer were analyzed by measuring the IR spectra. Figure 5a presents the IR spectrum of pure 1-butanol. Figure 5b illustrates the transition of the IR spectra of the alcohol polymer produced on the AFM tip (Fig. 1, white arrows). The change in the composition of the 1-butanol polymer was measured by recording the IR spectra at 30 min intervals (represented as different colors) over a three hour period. The red spectrum represents the signal recorded directly after the polymerization process. The black spectrum shows the composition of the polymer measured 3 h after its production.

The decomposition of 1-butanol molecules following electron bombardment (Fig. 6a) was confirmed by the transition of the IR spectra (Figs. 5a to 5b). The reduced peak size at 2959 and 2874 cm^{-1}, and the transition of the spectra between 1000 and 1500 cm^{-1} indicate that the C–H bonds in the 1-butanol molecules were decomposed (Fig. 6b). The broader peaks observed in Fig. 5b indicate the formation of 3-D bridge structures with the partially decomposed 1-butanol molecules (Fig. 6c).

The peak at 1720 cm^{-1} indicates the formation of C=O bonds in the 1-butanol polymer (Fig. 6c). The source of the oxygen in this reaction could be either the O–H bonds in the 1-butanol molecules or oxygen molecules in air. The peak could have originated from two different oxygen sources, although the ratio of their contributions is not known. Oxidation was often found to occur during the plasma-induced reactions.[17]

Two significant spectral transitions represented by the different colors can be observed in Fig. 5b. First is a simultaneous decrease of the signal at 3357 cm^{-1} and between 1000 and 1500 cm^{-1}. This decrease suggests the simultaneous evaporation of O–H and C–H bonds. It is therefore likely that 1-buta-

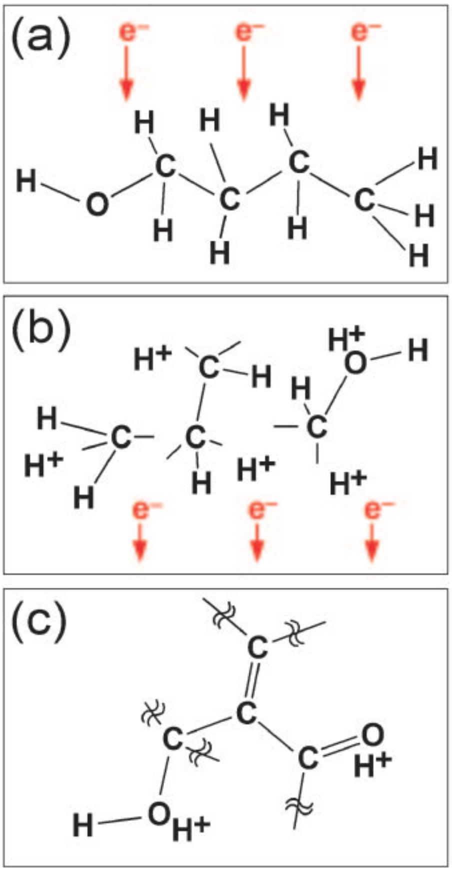

Fig. 6. Model of the dissociation process of 1-butanol molecules and possible structure of 1-butanol polymer. Electron emission to the 1-butanol molecule (a) dissociated the molecule (b) and composed 1-butanol polymer (c) from partially dissociated 1-butanol molecules (b).

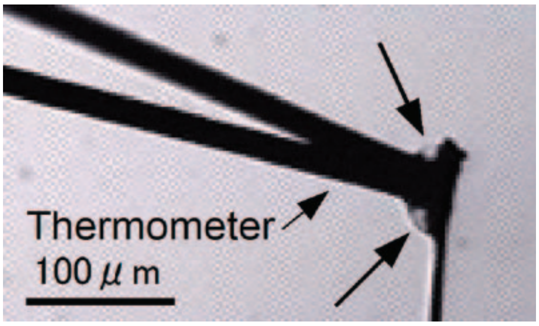

Fig. 7. Hydrogen production from the alcohol polymer and the simultaneous measurement of reaction temperature. An almel–cromel thermostat was used for applying electric potential and for measuring the reaction temperature.

nol, or partially decomposed 1-butanol molecules (Fig. 6b) should exist in the 1-butanol polymer, and might have evaporated from the polymer. Secondly is a rapid signal decrease from the red to green spectra between 1000 and 1500 cm^{-1}, compared to that of the 3357 cm^{-1} peak. The difference in the peak reduction ratio could reflect the structure of the evaporated species. If a 1-butanol molecule is evaporated, nine times the number of C–H bonds are disappeared compared with O–H bonds. This difference can be reflected in the IR spectra. Although an analysis of the evaporated material is not possible, based on the IR spectra alone, the differences in the ratios of the signal transition suggest the evaporation of 1-butanol, or partially decomposed 1-butanol molecules, from the polymer (Fig. 6b).

As another possibility, the significant spectrum transition between 1000 and 1500 cm^{-1} could be caused by the neutralization of hydrogen ions, and a subsequent production of hydrogen from the polymer (Fig. 6c). The properties of the plasma-induced reaction suggest that the mist produced on the AFM tip should be an amorphous polymer (Fig. 1, white arrows). The formation of the amorphous polymer required several 1-butanol molecules, and was shown to contain either C–C or C=C bonds for the formation of the 3-D structures (Fig. 6c). If nitrogen in air were dissociated, C–N bonds might also have contributed to the formation of the 3-D structure in the polymer (Fig. 10b).

Hydrogen Production from the Polymer. We also investigated the unstable composition of the 1-butanol polymer by measuring the resistivity. The resistivities of 1-butanol polymers are on the order of 10^{11}-Ω cm. However, the 1-butanol polymer reported here was found to have a resistivity that fluctuated between 0.8 and 480-Ω cm. This variation demonstrates that the 1-butanol molecules were decomposed. Interestingly, the resistivity of the 1-butanol polymer produced in this study was similar to the values obtained for most semiconductors. Similar resistivities have also been reported for other plasma-induced compounds.[18–20]

The unstable resistivity indicates that the polymer produced in this study was electrically unstable and in a non-equilibrium state. Figure 7 illustrates the AFM tip when an electrode with an electric signal of 6 V–50 Hz was applied directly to the polymer. When an electric signal was applied, the polymer began to produce bubbles at a rate of 670 μm^3/s (black arrows) and the bubble production continued for 5 s.

An almel–cromel thermometer was used to apply electric potential as an electrode, and for the simultaneous measurement of reaction temperature. The temperature of the polymer increased from 26 °C to 29 °C when an electric potential was applied, and bubbles were produced. The temperature remained at 29 °C for the duration of bubble production. Although a precise temperature measurement was difficult due to the size of the thermometer, the temperature of the bubbles was far less than the boiling point of the 1-butanol (117.3 °C). Therefore, the temperature increase should be caused by the enthalpy of gaseous formations, as observed in Fig. 7. The production and annihilation of the bubbles could be controlled by the applied electric potential.

The composition of the gas bubbles was measured by gas chromatography. The bubbles were found to consist of 18.5% hydrogen, 32% carbon dioxide, and 1.5% nitrogen. The composition of the remaining 48.5% could not be identified.

Structure and Electrical State of the Polymer. Several relationships were observed among the transition of the IR spectra between 1000 and 1500 cm^{-1} (Fig. 5b), the fluctuating electric resistivity of the polymer, and hydrogen production from the polymer (Fig. 7).

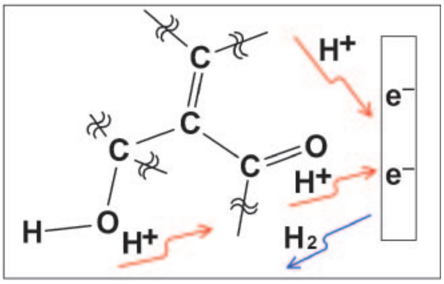

Fig. 8. Model of hydrogen production from the alcohol polymer. The hydrogen ions interacting with C=O and O–H bonds would be electrically attracted to the negative electrode and formed hydrogen at the electrode during the electrical neutrality.

The similarity between the electrical resistivity of the polymer produced in this study and many semiconductors indicates that certain charged particles, such as ions, could exist in the polymer and act as carriers. Hydrogen production by the polymer, following the application of an electric current, supports the idea that hydrogen ions act as both electrical carriers and as a source for hydrogen production (Fig. 8).

Hydrogen ions in the polymer should be present around the negatively charged species as a result of electrical interactions. The C=O or O–H bonds are the most likely sites for the interaction with hydrogen ions (Fig. 8). These polarized bases could potentially interact with hydrogen ions, causing the release of ions after the application of electrons from either an electric current or the AFM tip. The electrically neutralized hydrogen ions could then form hydrogen molecules (Fig. 8). The neutralization of hydrogen ions and subsequent production of hydrogen from the polymer might have caused the transition of the IR spectra between 1000 and 1500 cm^{-1}, as shown in Fig. 5b.

Mechanism of the Attenuation of Bubble Formation. The relationship between the attenuation of bubble production and the formation of an alcohol thin film on the AFM tip was investigated from the transition of IR spectrum of the alcohol polymer.

In our experiments (Fig. 7), bubble production was gradually decreased after 5 s. Since bubble production was caused by the application of an electric potential, there are two primary reasons why bubble formation was attenuated. First, all the hydrogen ions in the polymer were exhausted during the period. Second, the electron supply was inhibited. The latter case was supported by analyzing the polymer composed on the AFM tip, using a scanning electron microscope (SEM) in a vacuum.

Figure 9 represents a SEM image of an alcohol thin film composed on the AFM tip. The thin film appeared from the polymer on the tip (Fig. 1) when the electron emission in 15 kV of potential was applied with SEM in a vacuum. Before emission, the appearance of the polymer on the tip was spherical (Fig. 1, white arrows). However, after emission, a thin film was observed with SEM. During electron emission on the polymer, the image became blurred. These observations indicated that, initially the polymer was in the liquid state, which evaporated during the electron emission with SEM in a vacuum.

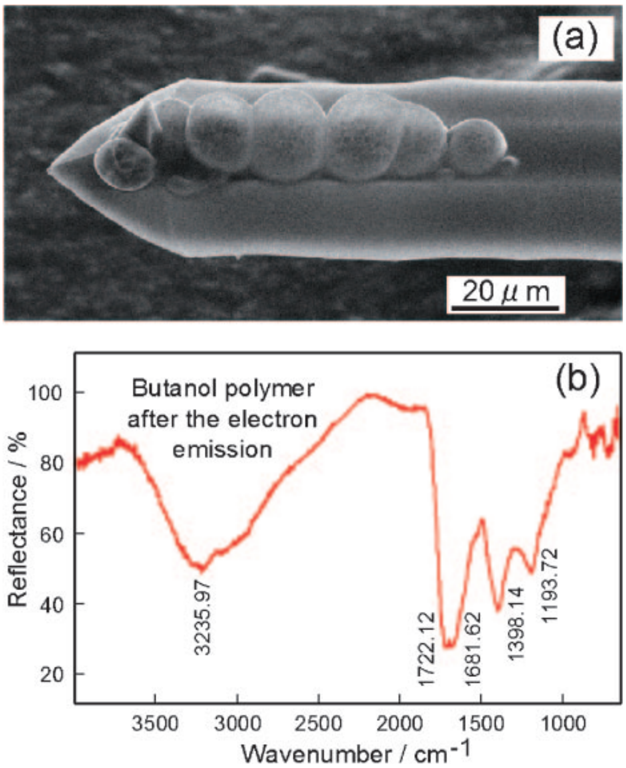

Fig. 9. Alcohol thin film and IR spectrum of the film. (a) Micro balloons composed from the alcohol thin film polymer. (b) IR spectrum of the alcohol polymer on the AFM tip in Fig. (a).

The alcohol thin film covering the AFM tip started to expand when the magnification of the SEM was increased to 2×10^4 times. After emission, several hemispherical micro balloons consisting of an alcohol thin film were observed. The micro balloons maintained their appearances while the tip was in a vacuum. These observations indicated that certain gasses would be contained in the micro balloons, and the film of the balloons was airtight at 10^{-3} Pa.

However, the balloons collapsed when the tip was taken out from the vacuum, possibly due to air pressure. This would indicate that the gas pressure in the balloons was much lower than the air pressure.

The evaporation of the liquid from the polymer and the structure of the alcohol thin film were analyzed from the IR spectrum in Fig. 9b.

Figure 9b represents an IR spectrum of alcohol thin film composing the micro balloons on the AFM tip in Fig. 9a. The disappearance of the 3357 and 1058 peaks in Fig. 5b indicated that the liquid polymer on the AFM tip initially contained 1-butanol or partially decomposed 1-butanol molecules. These molecules evaporated when electron emission with SEM was applied in a vacuum. The simultaneous appearances of 3235, 1681, and 1398 peaks in Fig. 9b correspond to the NH stretching, NH2 bending, and CN bending. These results indicated that the 1-butanol polymer on the AFM tip primarily consisted of a partially decomposed 1-butanol liquid polymer and alcohol thin film consisting of carbon, hydrogen, oxygen, and nitrogen (Fig. 10b).

The 1722 and 1681 peaks in Fig. 9b correspond to the 1720

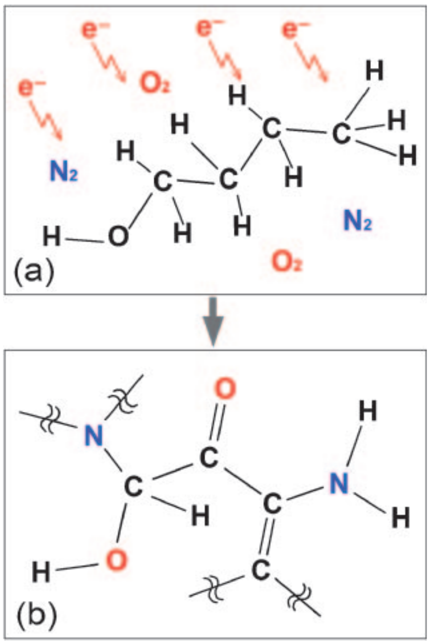

Fig. 10. Possible structure of alcohol thin film composed on the AFM tip in Fig. 9a. The simultaneous appearances of 3235, 1681, and 1398 peaks in Fig. 9b indicates that the alcohol thin film contains NH and CN bonds.

and 1668 peaks in Fig. 5b. If the estimation is correct, the signal decrease of 1720 indicates that some C=O bonds in the 1-butanol liquid polymer evaporated with electron emission with SEM in the vacuum. However, some C=O bonds contributed to the formation of the alcohol thin film (Fig. 10b).

The composition of the liquid 1-butanol polymer on the AFM tip (Fig. 1b, white arrows) could be estimated from the formation of an alcohol thin film consisting of nitrogen and the transition of the IR spectrum from Fig. 5b to Fig. 9b. The 1-butanol polymer composed on the AFM tip should have originally contained partially decomposed 1-butanol molecules, including at least NH and CN bonds. The nitrogen atoms in these bonds should be fixed from the air during electron bombardment. These ions including NH and CN should initially interact with other ions consisting of the liquid 1-butanol polymer. However, when an electric signal of 6 V–50 Hz was applied, these ions including NH and CN were stimulated to neutralize at the electrically opposite electrode. Since the almel–cromel thermometer was electrically insulated, these ions approached the AFM tip for their electrical neutrality. Therefore, an alcohol film consisting of nitrogen was composed on the AFM tip (Fig. 10).

The formation of the alcohol thin film would therefore be related to the attenuation of bubble production from the polymer on the AFM tip (Fig. 7). If semiconducting or insulating thin films were not formed on the AFM tip in Fig. 7, the electric potential applied from the thermometer would generate an electric current inside the polymer, and hydrogen would be produced from its ions. However, once the alcohol thin film was composed on the AFM tip, the electron supply would be stopped and hydrogen could not be formed from its ions. Therefore, the formation of an alcohol thin film on the AFM tip should be one of the reasons why bubble production was reduced.

These observations and analysis suggest that the insulating thin films sometimes worked unfavorably. However, insulating or semiconducting films are useful for storing hydrogen ions. In particular, one of the benefits of this method is an easier extraction of hydrogen. The hydrogen ions can be easily extracted from the insulating container with the application of an electric current. However, for engineering usage, a more detailed analysis of the electrical state of hydrogen ions in the insulating or semiconducting container would be necessary.

Summary

In this study, we investigated the dynamics of dielectric 1-butanol molecules interacting with electrons emitted from an intense electric field. The production of a nanoscale mist and microscale particles suggested an unstable electric state of the molecules. During this interaction, a 1-butanol polymer was produced on the electrode. The unstable structure of this polymer was investigated by measuring the transition of the IR spectrum, electric resistivity, and the production of hydrogen. The results indicated that the polymer was in a quasi-stable state and hydrogen was produced from hydrogen ions trapped inside the polymer.

The control of the stable structure for the storage of hydrogen ions and simultaneous unstable structure for the extraction of hydrogen is necessary for hydrogen storage and producing polymer. The insulating or semiconducting properties could also affect the storage efficiency and the extraction of hydrogen from the polymer. From this standpoint, the hydrogen-storing polymer composed from 1-butanol requires improvements. However, the storage of hydrogen in the form of ions could be a useful approach to hydrogen storage, since ions can easily be extracted by the application of an electric potential.

In future studies, we will investigate methods for improving the qualities of the hydrogen storage and producing polymers. The storage of hydrogen in the form of ions in other materials will also be investigated.

We thank K. Kondo, N. Higashi, M. Komatsu, and S. Ushiba for helpful discussions. This work was supported by Grants-in-Aid from the Intelligent Systems Institute, National Institute of Advanced Industrial Science and Technology.

References

1 E. Miller, R. E. Rocheleau, and S. Khan, *Int. J. Hydrogen Energy*, **29**, 907 (2004).

2 K. Gurunathan, *Int. J. Hydrogen Energy*, **29**, 933 (2004).

3 Z. Yumurtaci and E. Bilgen, *Int. J. Hydrogen Energy*, **29**, 687 (2004).

4 T. Sato, H. Blomqvist, and D. Noreus, *J. Alloys Compd.*, **356**, 494 (2003).

5 Y. Liu, H. Pan, Y. Zhu, R. Li, and Y. Lei, *Mater. Sci. Eng., A*, **372**, 163 (2004).

6 M. Conte, P. P. Prosini, and S. Passerini, *Mater. Sci. Eng., B*, **108**, 2 (2004).

7 M. Shiraishi, T. Takenobu, A. Yamada, M. Ata, and H. Kataura, *Chem. Phys. Lett.*, **358**, 213 (2002).

8 H. G. Schimmel, G. Nijkamp, G. J. Kearley, A. Rivera, K. P. de Jong, and F. M. Mulder, *Mater. Sci. Eng., B*, **108**, 124

(2004).

9 D. Luxembourg, G. Flamant, A. Guillot, and D. Laplaze, *Mater. Sci. Eng., B*, **108**, 114 (2004).

10 H. Matsuura, T. Tanikawa, H. Takaba, and Y. Fujiwara, *J. Phys. Chem. A*, **108**, 3235 (2004).

11 P. E. Slade, Jr. and L. T. Jerkins, "Thermal Characterization Techniques," Marcel Dekker, Inc., New York (1970).

12 E. S. Gould, "Mechanism and Structure in Organic Chemistry," Holt, Rinehart, Winston, New York (1960).

13 R. T. Morrison and R. N. Boyd, "Organic Chemistry," 6th ed, Prentice Hall, Englewood Cliffs, New Jersey (1992).

14 L. B. Clapp, "The Chemistry of the OH Group," Pentice-Hall, Inc., Englewood Cliffs, New Jersey (1967).

15 L. Pauling, "The Nature of the Chemical Bond," 3rd ed, Cornell University Press, New York (1960).

16 R. J. Gillespie, *J. Chem. Educ.*, **40**, 295 (1963).

17 H. V. Boenig, "Advances in Low Temperature Plasma Chemistry, Technology, Applications," Technomic Publishing, Pennsylvania (1984).

18 A. Bradley and J. P. Hammes, *J. Electrochem. Soc.*, **110**, 543 (1963).

19 J. Guastavino, H. Carchano, and A. Bui, *Thin Solid Films*, **24**, S23 (1974).

20 C. K. Chiang, M. A. Pruy, S. C. Gan, A. J. Heeger, E. J. Louis, A. G. MacDiarmid, Y. W. Park, and H. Shirakawa, *J. Am. Chem. Soc.*, **100**, 1013 (1978).